Multireference calculations on low-lying states and the $X^3\Pi_u$–$^3\Pi_g$ absorption spectra of indium dimers*

Zhou Ling-Song(周凌松), Yan Bing(闫 冰)†, and Jin Ming-Xing(金明星)

Institute of Atomic and Molecular Physics, Jilin University, Changchun 130012, *China*

(Received 13 July 2012; revised manuscript received 3 September 2012)

Multireference configuration interaction calculations are carried out on 11 Λ–S low-lying electronic states of indium dimers. The Ω states are investigated with spin–orbit pseudopotentials via the state-interacting method, and characterized by fitted spectroscopic constants based on computed potential energy curves. The vibrational structures of the double-potential well 0_g^+(I) ($^3\Sigma_g^-$) state are also analyzed. The experimentally observed absorption spectrum centred at ∼ 13000 cm^{-1} is simulated and assigned to $X^3\Pi_u$ ($v' = 0$)–$^3\Pi_g$ transition according to the present *ab initio* calculations on transition energies and dipole moment functions.

Keywords: indium dimer, spin–orbit coupling, spectroscopic constants, transition dipole moment

PACS: 31.50.DF, 33.15.Mt, 32.70.Cs, 31.30.J– **DOI:** 10.1088/1674-1056/22/4/043102

1. Introduction

Metal[1–4] and non-metal[5–7] clusters have aroused much interest in theoretical computations and experiments. Compared with the group 3A metal dimmers B_2, Al_2, and Ga_2, the indium dimer (In_2) has not been well characterized in previous investigations. Experiments on In_2 have not been very intensively conducted. The gas phase electronic spectra of In_2 were observed in the King furnace in early experiments.[8] Douglas *et al*.[9] reported on two electronic absorption bands of In_2 isolated in cryogenic matrices, with the peaks at 13000 cm^{-1} and 27691 cm^{-1}. While the absorption centred at 13000 cm^{-1} was incorrectly assigned to $^1\Pi_u$–$^1\Sigma_g^+$ transition. Electronic transitions in the range 25500 cm^{-1}–27000 cm^{-1} were then observed in indium vapor and were assigned to $^3\Pi_g$(II)–$X^3\Pi_u$. The ground-state harmonic vibrational frequency and anharmonic constant were assigned by Raman spectra of the matrix-isolated In2 as $\omega_e = 118$ cm^{-1}, $\omega_e x_e = 0.8$ cm^{-1}, respectively.[10] Balasubramanian and Li[11] calculated the potential energy surfaces of the low-lying electronic states of In_2 using the complete active space multiconfigurational self-consistent field method and first-order configuration interaction method, and reported on the spectroscopic properties of some electronic states. According to the calculated transition energy, the absorption spectrum at 13000 cm^{-1} was reassigned to $X^3\Pi_u$–$^3\Pi_g$ transition.

In the present work, firstly the main spectroscopic constants (equilibrium bond distance r_e, harmonic frequency ω_e, anharmonic frequency $\omega_e x_e$, rotational constant B_e, transition energy T_e) of bound Λ–S and Ω states of In_2 are calculated with the multireference configuration interaction method. Secondly, the irregular vibrational progression of the double-potential well 0_g^+(I) state is analyzed, and finally the transition dipole moment functions of the branch transitions in $X^3\Pi_u$–$^3\Pi_g$ are reported, and the $X^3\Pi_u$ ($v = 0$)–$^3\Pi_g$ absorption spectra are simulated. Comparisons between the available experimental results and the computation results are then made.

2. Theoretical methods

The relativistic multiconfiguration Dirac–Hartree–Fock (DHF) pseudopotential[12] for 28 core electrons ($1s^2 2s^2 2p^6 3s^2 3p^6 3d^{10}$) in combination with the quadruple-zeta basis set[13] (15s12p13d3f2g)/[7s7p5d3f2g] for valence electrons is used to describe the In atom. The computations are performed in the D_{2h} subgroup instead of the $D_{\infty h}$ point group. In D_{2h} symmetry, Σ_g^+=A_g, Σ_u^+=B_{1u}, Σ_g^-=B_{1g}, Σ_u^-=A_u, Π_g=B_{2g}+B_{3g}, and Π_u=B_{2u}+B_{3u}. The lowest 11 electronic states, the singlet $\Sigma_g^+(2)$, Σ_u^-, $\Pi_{g,u}$, Δ_g, and triplet Σ_g^-, Σ_u^+, $\Pi_{g,u}$, Δ_u states, correlating to the first dissociation limit In(^{2}P)+In(^{2}P), are included in the present *ab initio* calculations. The state-averaged valence completed active space multiconfigurational self-consistent field (SA-CASSCF) method is used to generate reference wavefunctions, and the dynamical correlations are computed by the internally contracted singly and doubly excitation multireference configuration interaction method[14] (icMRCISD) with Davidson correction[15] (+Q) to account for the higher order excitation configurations.

The spin–orbit coupling is introduced by a spin–orbit pseudopotential via the state-interaction method. The spin–orbit eigenstates are obtained by diagonalizing the Hamiltonian $H_{el} + H_{SO}$ on the basis of the eigenfunctions of H_{el}, in which H_{el} is the unperturbed Hamiltonian and H_{SO} is the spin–orbit Hamiltonian as perturbation. The diagonal spin–orbit

*Project supported by the National Magnetic Confinement Fusion Science Program of China (Grant No. 2010GB104003) and the Fundamental Research Funds for the Central Universities (Grant No. 450060481375).

†Corresponding author. E-mail: yanbing@jlu.edu.cn

© 2013 Chinese Physical Society and IOP Publishing Ltd

matrix elements are replaced by the icMRCISD+Q energies of the Λ–S states, and the zero-order eigenfunction basis is calculated with the icMRCISD method.

For comparison, the geometries of the lowest singlet and triplet states are also optimized by using the single, double, and perturbative triple excitation coupled cluster theory and the icMRCISD method combined with the relativistic full-electron basis set ANO-RCC.[16] In couple cluster computation in the ground state, the spin-restricted Hartree–Fock (open) closed shell wavefunctions are used as reference. That is, the RHF-(U)CCSD(T) method[17] is used for first (triplet) singlet state in this work. The molecular orbitals corresponding to the $n = 1 \sim 4$ atomic orbitals are kept uncorrelated in both the RHF-(U)CCSD(T) and icMRCISD computations. The scalar relativistic corrections are included in the RHF-(U)CCSD(T)/ANO-RCC and icMRCISD/ANO-RCC computations by using the Douglas–Kroll–Hess (DKH) Hamiltonian.[18–20] The harmonic frequency of the ground state is numerically calculated at the RHF-(U)CCSD(T)/ANO-RCC level. All electronic structure calculations are performed with the Molpro[21] package.

3. Results and discussion

3.1. Λ–S states

The spin-free potential energy curves of 11 Λ–S states computed with the icMRCISD+Q method are illustrated in Fig. 1, and the corresponding spectroscopic constants are listed in Table 1. The ground state $X^3\Pi_u$ arises from the $5s\sigma_g^2g5s\sigma_u^2g5p\sigma_g^1g5p\pi_u^1$ configuration. In a previous report,[9] the ground state of In_2 is wrongly assigned to the $^1\Sigma_g^+$ state with a $5s\sigma_g^2g5s\sigma_u^2g5p\sigma_g^2$ configuration. The present computations demonstrate that the $5p\sigma_g$ and $5p\pi_u$ orbital are nearly degenerate, and thus the triplet ground state with two parallel-spin electrons distributing into the nearly degenerate $5p\sigma_g$ and $5p\pi_u$ orbital tends to reduce Pauli repulsion, while for the singlet $^1\Sigma_g^+$ state with two antiparallel-spin electrons in $5p\sigma_g$ orbital, the Pauli repulsion interaction increases. The lowest $^1\Sigma_g^+$ state, which arises mainly from the $5s\sigma_g^2g5s\sigma_u^2g5p\sigma_g^2$ (70%) configuration with a mixture of the $5s\sigma_g^2g5s\sigma_u^2g5p\pi_u^2$ (30%) configuration in equilibrium geometry, is 1300 cm^{-1} higher than the $X^3\Pi_u$ state; the triplet $^3\Sigma_g^-$ state, which arises mainly from $5s\sigma_g^2g5s\sigma_u^2g5p\pi_u^2$ (80%), lies 60 cm^{-1} under the singlet $1^1\Sigma_g^+$ state; the singlet–triplet energy gap between the two states should be attributed to the Pauli exclusion principle taking effect in the $5p\pi$ orbital.

Our calculated r_e of ground state $X^3\Pi_u$ is 3.068 Å (1 Å = 0.1 nm), the ω_e, $\omega_e x_e$, and B_e are 114.7, 0.2907, and 0.0312 cm^{-1}, respectively. As listed in Table 1, the computed values of r_e in the previous literature are 3.13 Å[11] with the first-order CI method and 2.97 Å[16] with the second-order perturbation theory, which differ from each other by as much as ~ 0.16 Å. Our computed values are 3.068 Å at the icMRCISD+Q/pseudopotential level, 3.085 Å by the RHF-UCCSD(T) method with full-electron basis set, and 3.087 Å by the icMRCISD with full-electron basis. The present computed values from different methods and basis sets accord well with each other within 0.02 Å. Less than 1 cm^{-1} errors are found between our computed values of ω_e and the previous theoretical value.[11]

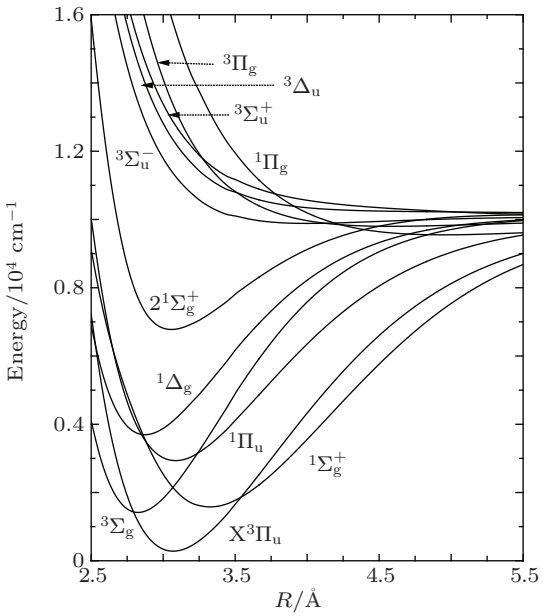


Fig. 1. The potential energy curves of the Λ–S states.

Table 1. Spectroscopic constants for the low-lying Λ–S states of In_2.

States	Reference	T_e	r_e	ω_e	$\omega_e x_e$	B_e
$X^3\Pi_u$	present	0	3.068	114.7	0.2907	0.0312
	present		3.085[a]	114.3[a]		
	present	0	3.087[b]	–		
	Ref. [11]	0	3.13	114		
	Ref. [16]	0	2.970	120		
$^3\Sigma_g^-$	present	1129.2	2.824	140.3	0.4524	0.0368
	Ref. [11]	1043	2.87	142		
$1^1\Sigma_g^+$	present	1300	3.325	89.6	0.0190	0.0265
	present	1495[a]	3.347[a]	95.5[a]		
	present	1840[b]	3.340[b]	–		
	Ref. [11]	4149	3.29	91		
$^1\Pi_u$	present	2653.0	3.085	110.9	0.3179	0.0308
	Ref. [11]	3666	3.20	98		
$^1\Delta_g$	present	3410.2	2.871	128.1	0.6619	0.0356
	Ref. [11]	4195	2.98	109		
$2^1\Sigma_g^+$	present	6496.2	3.055	109.0	0.5890	0.0314
	Ref. [11]	7371	3.29	89		

[a] CCSD(T)/ANO-RCC in this work; [b] MRCI/ANO-RCC in this work

For the lowest singlet state $^1\Sigma_g^+$, our calculated values of r_e are 3.325 Å with the icMRCISD+Q and relativistic pseudopotential, and 3.347 Å at the RHF-CCSD(T)+DK/ANO-RCC level. Our calculated values are consistent with each other within 0.022 Å, and close to the previous theoretical value 3.29 Å.[11] Our calculated value of ω_e is also in good accordance with the previous value.[11] Though in the configurations for the lowest two excited states, the $5s\sigma_g^2g5s\sigma_u^2g5p\sigma_g^2$

and $5s\sigma_g^2g5s\sigma_u^2g5p\pi_u^2$ components both exist, and the values of r_e for the $^3\Sigma_g^-$ and $^1\Sigma_g^+$ states differ by as much as ~ 0.5 Å, both in ours and the previous computations. The $5p\sigma_g^2$ and $5p\sigma_u^2$ orbital are of antibonding and bonding natures, respectively, and the percentage of the $5s\sigma_g^2g5s\sigma_u^2g5p\pi_u^2$ configuration for the triplet state is larger than that for the singlet, so the triplet state $^3\Sigma_g^-$ is more bonding than the singlet state $^1\Sigma_g^+$.

The same configurations as the $X^3\Pi_u$ state but with opposite spin for two singly-occupied electrons gives rise to the first singlet Π_u state, which lies at 2653.0 cm^{-1} above the ground state. The spectroscopic constants are similar to those of the ground state; it is worth noting that the value of r_e of the $^1\Pi_u$ state is increased by 0.017 Å due to the Pauli repulsion interaction compared with that of the ground state. The electronic transition from $5p\sigma$ to $5p\pi_u$ gives rise to the $^1\Delta_g$ state, and the $5p\pi_u$ orbital is then doubly occupied. The $^1\Delta_g$ state has a similar configuration to the $^3\Sigma_g^-$ state, with different spin and angular coupling schemes. The $^1\Delta_g$ state with r_e of 2.871 Å lies at 3410.2 cm^{-1} above the ground state, and the values of ω_e, $\omega_e x_e$, and B_e are 128.1, 0.6619, and 0.0356 cm^{-1}, respectively. The highest bound state involved in this work is the second $^1\Sigma_g^+$ state lying at 6496.2 cm^{-1} above the ground state. For the $2^1\Sigma_g^+$ state, our calculated values of ω_e, $\omega_e x_e$, and B_e are 109.0, 0.5890, and 0.0314 cm^{-1}, respectively.

To the best of our knowledge, no experimental value of T_e for the bound state is available for comparison. Fortunately, the vertical transition energy (VTE) from $X^3\Pi_u$ to $^3\Pi_g$ has been measured by experimental absorption spectra to be 13000 cm^{-1}. The previously calculated VTE of $X^3\Pi_u$–$^3\Pi_g$ is 12423 cm^{-1}, which deviates from the experimental value by 573 cm^{-1}. The calculated VTE value is then improved to be 13089 cm^{-1} by the icMRCI+Q method in our computations, and the relative error is reduced from 4.41% to 0.68%, which indicates that our theoretical methods in this work are accurate enough to predict transition energies. As listed in Table 1, our calculated transition energy of the first excited state $^3\Sigma_g^-$ is 1130 cm^{-1}, which is only 86 cm^{-1} higher than the previously calculated value.[11] While for the $1^1\Sigma_g^+$ state, our calculated T_e conflicts with the previously calculated one. In previous computational work, the predicted energy order for the $1^1\Sigma_g^+$ and $^1\Pi_u$ states is $1^1\Sigma_g^+ > {}^1\Pi_u$,[11] while our icMRCISD+Q computations give an inverse energy order. The previously calculated T_e of $1^1\Sigma_g^+$ state is 4149 cm^{-1},[11] which differs from our calculated value 1300 cm^{-1} with the icMRCI+Q/pseudopotential by 2850 cm^{-1}. Our calculated values of T_e for the $1^1\Sigma_g^+$ state at RHF-CCSD(T)/ANO-RCC and the icMRCISD/ANO-RCC level are 1495 cm^{-1} and 1840 cm^{-1}, respectively, and our calculated values at different levels are consistent within a few hundreds cm^{-1} error, which reveals that our calculated T_e for $^1\Sigma_g^+$ is more secure than the previous one. In addition, the T_e energy order in isovalent molecule Ga_2 was found to be $1^1\Sigma_g^+ < {}^1\Pi_u$ in previous work,[22] which is consistent with our present computations for In_2. The previous $1^1\Sigma_g^+ - {}^1\Pi_u$ energy gap of In_2 is -483 cm^{-1},[11] and in contrast, the present value is 1353 cm^{-1}, which is reasonably close to that in the Ga_2 molecule, 911 cm^{-1}[22] in the previous work. For the other three higher states, $^1\Pi_u$, $^1\Delta_g$, and $2^1\Sigma_g^+$, the difference between our calculated T_e and the previous ones are in a range of 800 cm^{-1}–1000 cm^{-1} (0.1 eV$\sim$ 0.12 eV), which are typical errors in multireference calculations, so no further computational efforts are made in the present work.

3.2. Ω states

The calculated electronic curves with the inclusion of spin–orbit coupling are shown in Figs. 2 and 3, respectively, for $\Omega = 0^+$, 0^- and $\Omega = 1$, 2. The spectroscopic parameters for the bounding Ω states are listed in Table 2. According to Wigner–Witmer correlation rules, the 0_g^+, 0_u^-, and 1_u Ω states are correlated with the $In(^2P^o_{1/2}) + In(^2P^o_{1/2})$ limit, the 2_u, 2_g, $1_u(2)$, $1_g(2)$, 0_g^+,0_u^+, 0_g^-, and 0_u^- states are correlated with the second dissociation limit $In(^2P^o_{1/2}) + In(^2P^o_{3/2})$, and the third atomic limit $In(^2P^o_{3/2}) + In(^2P^o_{3/2})$ gives rise to the 3_u, 2_u, 2_g, $1_u(2)$, 1_g, $0_g^+(2)$, $0_u^-(2)$ states. Our calculated spin–orbit splittings for the first-second and second-third atomic limits at an internuclear distance of $R = 20.0$ Å are 0.22 eV, and 0.23 eV, respectively, which are both close to experimental atomic $In(^2P^o_{1/2})$–$In(^2P^o_{3/2})$ splitting 0.27 eV.[23] The $X^3\Pi_u$ state splits into four Ω components, 0_u^+, 0_u^-, 1, and 2_u, in which the $\Omega = 0_u^-$ state is the lowest one. Compared with the Λ–S ground state $X^3\Pi_u$, the spin–orbit coupling leads to a reduction in the equilibrium bond distance r_e by 0.003 Å$\sim$0.006 Å for $\Omega = 0_u^-$ and 0_u^+, while it gives an elongation of r_e by 0.002 Å$\sim$0.006 Å for the $\Omega = 1_u$ and 2_u states. The values of our calculated ω_e, $\omega_e x_e$, and B_e for the Ω components of the ground state differ correspondingly little from the above. In particular, for the ground state $0_u^-(I)$, our calculated values of ω_e and $\omega_e x_e$ are closer to the experimental values from the Raman spectra[10] than the previous computation values.[11] Both ours and the previous computations give the same energy order for the Ω components of the ground state, though small differences between ours and the previous computations[11] are found to be in a range of 140 cm^{-1}–400 cm^{-1} (0.02 eV$\sim$0.05 eV) for the calculated SOC splitting in the $X^3\Pi_u$ state. The $^3\Sigma_g^-$ state splits into the $0_g^+(I)$ and $1_g(I)$ Ω states, and the calculated values of T_e in this work and the previous literature[11] are consistent within ~ 200 cm^{-1}. Two energy minima are found in the $0_g^+(I)$ potential, which are located at 2.834 Å and 3.312 Å, respectively. A large discrepancy between this computation and the previous result[11] for the $1^1\Sigma_g^+$ state, which has been discussed above, leads to different values of T_e and the spectroscopic constants of the $0_g^+(II)$ state. The contributions to the bound $1_u(II)$, 2_g, and $0_g^+(III)$ Ω states are mainly made by the $^1\Pi_u$, $^1\Delta_g$, and $2^1\Sigma_g^+$ Λ–S states, respectively. By comparing with the T_e of the Λ–S states, the spin–orbit interaction is found to lift the Ω state by several hundreds of cm^{-1}, while there is little change for the spectroscopic constants.

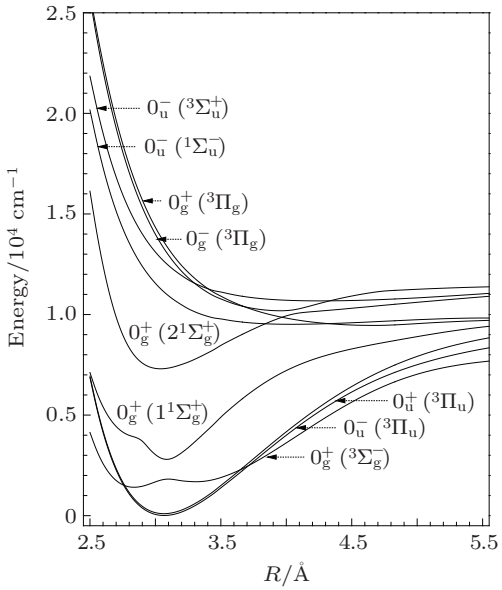


Fig. 2. The potential energy curves of the $\Omega = 0$ states.

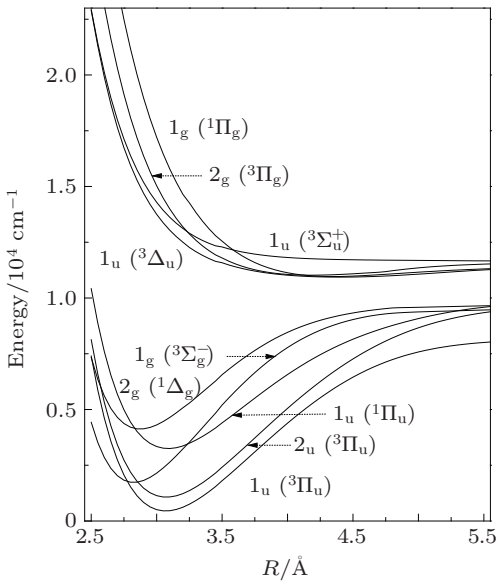


Fig. 3. The potential energy curves of the $\Omega = 1$ and 2 states.

Table 2. Spectroscopic constants for the Ω states of In_2.

Ω states (Λ–S states)		T_e	r_e	ω_e	$\omega_e x_e$	B_e
0_u^-(I) ($^3\Pi_u$)	present	0	3.065	114.5	0.3012	0.0312
	Expt. [10]	–	–	118	0.8	
	Ref. [11]	0	3.14	111		
0_u^+(I) ($^3\Pi_u$)	present	90.7	3.063	115.0	0.2989	0.0313
	Ref. [11]	231	3.12	114		
1_u(I) ($^3\Pi_u$)	present	451.6	3.070	114.0	0.2947	0.0311
	Ref. [11]	625	3.13	113		
2_u ($^3\Pi_u$)	present	1071.2	3.074	114.1	0.2829	0.0311
	Ref. [11]	1397	3.14	113		
0_g^+(I) ($^3\Sigma_g^-$)	present	1399.8	2.834	104.9	3.8449	0.0365
	present	1682.6	3.312	81.7	−1.7854	0.0269
	Ref. [11]	1444	2.89	132		
1_g(I) ($^3\Sigma_g^-$)	present	1730.7	2.8240	140.0	0.4592	0.0368
	Ref. [11]	1947	2.88	141		
0_g^+(II) ($1^1\Sigma_g^+$)	present	2771.7	3.0848	192.7	4.8381	0.0308
	Ref. [11]	5112	3.29	91		
1_u(II) ($^1\Pi_u$)	present	3250.1	3.0882	110.2	0.3251	0.0308
	Ref. [11]	4701	3.20	98		
2_g(I) ($^1\Delta_g$)	present	4124.8	2.8738	127.4	0.6684	0.0355
	Ref. [11]	5158	2.98	109		
0_g^+(III) ($2^1\Sigma_g^+$)	present	7292	3.0372	112.4	0.6308	0.0318
	Ref. [11]	8334	3.29	89		

3.3. The vibrational structures of the double-well 0_g^+(I) ($^3\Sigma_g^-$)

As listed in Table 2, the double minima for the 0_g^+(I) ($^3\Sigma_g^-$) potential are located at 2.834 Å and 3.312 Å, and the barrier between the two minima is 0.0535 eV relative to the bottom in the inside of the potential well with the maximum point located at 3.098 Å. The lowest 10 vibrational levels ($v = 0 \sim 9$) in the 0_g^+(I) potential are shown Fig. 4. The vibrational states of $v = 0$, 1 are exclusively localized inside the potential well. The $v = 2$, 3 states are nearly degenerate due to the presence of a second potential well, and largely localized inside the potential well, with only a very small probability outside the potential well ($v = 3$ in Fig. 4). As shown in Fig. 4, the $v = 4$ state is largely localized inside the potential well, while the probability inside the potential well is non-negligible. Tunneling from the inside to the outside of the potential well occurs for the $v = 4$ vibrational wavefunction. The $v = 5$ state, though it lies below the potential maximum, is delocalized due to strong tunneling between the inside and the outside of the potential well. The $v > 5$ states, which all lie above the potential maximum, are completely delocalized.

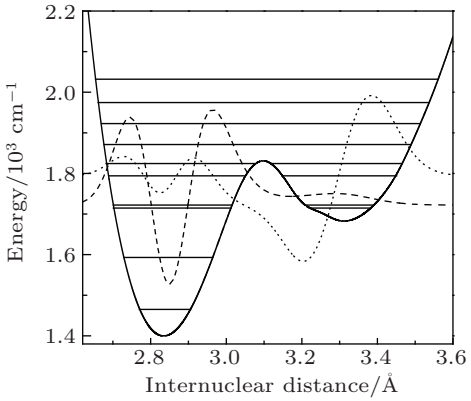


Fig. 4. The potential energy curves of the 0_g^+(I) and wavefunctions (in arbitrary amplitudes) of $v = 3$ (dashed curve) and $v = 4$ (dotted curve).

3.4. $X^3\Pi_u(v' = 0)$–$^3\Pi_g$ absorption spectra

A strong transition centred at 13000 cm^{-1} was found in the experimental absorption spectrum, which was wrongly assigned to the $^1\Sigma g^+$–$^1\Pi_u$ transition.[9] Subsequently, the absorption spectrum was assigned to the $^3\Pi_u$–$^3\Pi_g$ transition, and the transition energy was calculated to be 12423 cm^{-1},[11] while the transition properties were lacking for the absorption spectra. The three branch transitions 2_u–1_g, 0_u^-–0_g^-, and 1_u–0_g^+ in the $X^3\Pi_u$–$^3\Pi_g$ transition were simulated and the results are shown in Fig. 5. The characterized parameters of the simulated absorption spectra are listed in Table 3. The transition dipole moment (TDM) functions of the branch transitions have similar shapes, with the maxima in a range of 3.3 Å∼3.35 Å. The maximal TDM is ∼ 1.27 a.u. (1 a.u. = 2.542 deb, 1 deb=3.33564×10^{-30} C·m). The absorption spectra are assumed to be contributed from the $v = 0$ vibrational state of the $X^3\Pi_u$ state in this work. The branch absorption spectra of the $X^3\Pi_u(v = 0)$–$^3\Pi_g$ absorption spectra almost coincide with each other, and the spectrum peaks are at 13133, 13091, and 13075 cm^{-1}, respectively. The full width at half maximum (FWHM) values of the branch transitions are less than 1200 cm^{-1} and larger than 400 cm^{-1}, but smaller than the experimental values. The total absorption spectra are estimated by summing the branch spectra with equal weight. The spectrum peak value accords with the experimental result within 1% error, and is in good agreement with the previous computations. It is reasonable that our calculated FWHM is smaller than the experimental value[11] as the other spectrum broadening mechanism is not considered in this work. As a result, our present computations of the transition properties confirm that the absorption at 13000 cm^{-1} belongs to the $X^3\Pi_u$–$^3\Pi_g$ transition.

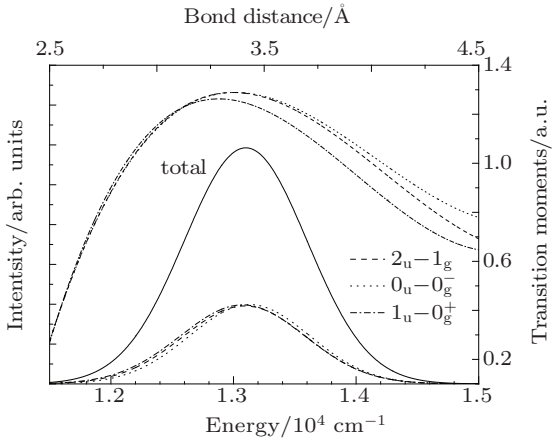


Fig. 5. The transition dipole moment functions (top and right axes) and absorption spectra (bottom and left axes) in the $X^3\Pi_u(v' = 0)$–$^3\Pi_g$ transition.

Table 3. The absorption spectra of the $X^3\Pi_u$–$^3\Pi_g$ transitions.

Transition	Peak	FWHM
$2_u(X^3\Pi_u)$–$1_g(^3\Pi_g)$	13133	1154
$0_u^-(X^3\Pi_u)$–$0_g^-(^3\Pi_g)$	13091	1181
$1_u(X^3\Pi_u)$–$0_g^+(^3\Pi_g)$	13075	1196
Total	13100	1179
Expt. [9]	13000±15	1600
Ref. [11]	12423	–

4. Conclusion

In the present work, we report on the main spectroscopic constants of the low-lying electronic states of In_2 molecules. The relativistic core potential, together with a large molecular basis set and valence configuration interactions, are used to characterize the low-lying electronic states. The vibrational levels in the double-potential well of the 0_g^+(I) ($^3\Sigma_g^-$) state show irregular progression, and tunneling is found to exist between the inside and the outside of the potential well for the $v = 3, 4$ levels. The absorption spectra of $X^3\Pi_u(v{=}0)$–$^3\Pi_g$ are simulated based on calculated Ω state potentials and transition dipole moment functions. Some improved spectroscopic constants of the bound states are suggested in this work.

References

[1] Balasubramanian K 1990 *Chem. Rev.* **90** 93
[2] Lu Y and Chen W 2012 *Chem. Soc. Rev.* **41** 3594
[3] de Heer W A 1993 *Rev. Mod. Phys.* **65** 611
[4] Zhang C J, Hu B T and Luo X W 2012 *Chin. Phys. B* **21** 053601
[5] Zhang X N, Shi D H, Sun J F and Zhu Z L 2011 *Chin. Phys. B* **20** 43105
[6] Tong X F, Yang C L, Xiao J, Wang M S and Ma X G 2010 *Chin. Phys. B* **19** 123102
[7] Huang D H and Wanf F H 2009 *Acta Phys. Sin.* **58** 6091 (in Chinese)
[8] Ginter D S, Ginter M L and Innes K K 1965 *J. Phys. Chem.* **69** 2480
[9] Douglas M A, Hauge R H and Margrave J L 1983 *J. Phys. Chem.* **87** 2945
[10] Froben F W, Schulze W and Kloss U 1983 *Chem. Phys. Lett.* **99** 500
[11] Balasubramanian K and Li J 1988 *J. Chem. Phys.* **88** 4979
[12] Metz B, Stoll H and Dolg M 2000 *J. Chem. Phys.* **113** 2563
[13] Peterson K A 2003 *J. Chem. Phys.* **119** 11099
[14] Werner H J and Knowles P J 1988 *J. Chem. Phys.* **89** 5803
[15] Langhoff S R and Davidson E R 1974 *Int. J. Quantum Chem.* **8** 61
[16] Roos B O, Lindh R, Malmqvist P Å, Veryazov V and Widmark P O 2004 *J. Phys. Chem. A* **108** 2851
[17] Knowles P J, Hampel C and Werner H 1993 *J. Chem. Phys.* **99** 5219
[18] Wolf A, Reiher M and Hess B A 2002 *J. Chem. Phys.* **117** 9215
[19] Reiher M and Wolf A 2004 *J. Chem. Phys.* **121** 2037
[20] Reiher M and Wolf A 2004 *J. Chem. Phys.* **121** 10945
[21] Werner H J, Knowles P J, Knizia G, Manby F R and Schütz M 2012 *WIREs Comput. Mol. Sci.* **2** 242
[22] Das K K 1997 *J. Phys. B* **30** 803
[23] Kramida A, Ralchenko Yu, Reader J and NIST ASD Team 2012 *NIST Atomic Spectra Database* (version 5.0) http://physics.nist.gov/asd (National Institute of Standards and Technology, Gaithersburg, MD)